# Bethe-ansatz wave function, momentum distribution, and spin correlation in the one-dimensional strongly correlated Hubbard model

Masao Ogata* and Hiroyuki Shiba†
*Institute for Solid State Physics, University of Tokyo, Roppongi, Tokyo 106, Japan*
(Received 29 August 1989)

The momentum distribution function $n(k)$ and spin-correlation function $S(k)$ are determined for the one-dimensional large-$U$ Hubbard model with various electron densities. The present work is featured with an application of the Bethe-ansatz wave function, which has a simple form in the large-$U$ limit for any electron density. Namely, its charge degrees of freedom are expressed as a Slater determinant of spinless fermions, while its spin degrees of freedom are equivalent to the one-dimensional $S=\frac{1}{2}$ Heisenberg model. The singularity of $n(k)$ at $k=k_F$ is analyzed from the system size dependence. In addition to the $k_F$ singularity, $n(k)$ has a weak singularity at $k=3k_F$; however, no detectable singularity is present at $2k_F$, which one might expect from the spinless fermion wave function. The singularity of $S(k)$ at $2k_F$ is also examined in detail. It is concluded from the size dependence that, when the system is away from half-filling, the nature of the singularity at $2k_F$ is different from that in the Heisenberg model. The results are compared with the behavior in the weak-correlation regime examined with the perturbation calculation, the prediction of $g$-ology, and recent Monte Carlo calculations.

## I. INTRODUCTION

The Hubbard model is the simplest Hamiltonian containing the essence of strong correlation. Recently it has attracted much attention again in connection with the high-$T_c$ superconductivity.[1] Although the doped carriers in high-$T_c$ superconductors mainly occupy oxygen $p$ orbitals in the two-dimensional $CuO_2$ plane, the strongly correlated Hubbard model is often used as an effective Hamiltonian.[2,3]

Notwithstanding its apparent simplicity, our understanding of the physics of the Hubbard model is still limited. Even in the one-dimensional case[4] our knowledge is far from complete. In fact, although its thermodynamics was clarified by many authors,[4,5] various important quantities such as momentum distribution and correlation functions, which require an explicit form of the wave function, have not been explored yet.

The purpose of this paper is to present the momentum distribution and spin-correlation function in the large-$U$ limit of the one-dimensional Hubbard model based on the exact Bethe-ansatz wave function. To this end we first observe that the Lieb and Wu wave function[4] has a very simple form in the large-$U$ limit owing to a decoupling of charge and spin degrees of freedom. Namely, in the large-$U$ limit the charge degrees of freedom of the ground state are expressed as a Slater determinant of spinless fermions, while its spin degrees of freedom are equivalent to the one-dimensional $S=\frac{1}{2}$ Heisenberg model.[6] This notable feature holds for any electron density. A similar decoupling has been used recently to study the two-hole state in connection with Nagaoka's ferromagnetism.[7] This observation enables us to calculate exactly the momentum distribution $n(k)$ and spin-correlation function $S(k)$ in the strong-correlation regime, which are not available in other methods. In practice the calculation is carried out for large but finite systems up to 32 sites.

Both the momentum distribution function $n(k)$ and spin-correlation function $S(k)$ are interesting quantities, especially for strongly correlated systems. First of all, we can learn through $n(k)$ how the dynamics of electrons (or holes) is affected by surrounding spins. For example, one might expect from the spinless fermion wave function that the momentum distribution may have a singularity at $k=2k_F$. As we shall show, rearrangements of spin configurations in the hopping process play an essential role to smear out the $2k_F$ singularity, leading to a singularity at $k_F$ instead. Secondly, the momentum distribution is also related to the problem of whether the low-energy states in the strongly correlated Hubbard model ($t$-$J$ model) can be represented by a Fermi liquid or not.[1] Recently, Sorella *et al.*[8] have developed a new algorithm of Monte Carlo simulation and studied the momentum distribution, which has renewed our interest in this quantity. Thirdly, contrary to a sharp jump of $n(k)$ at $k=k_F$, that is characteristic to the ordinary Fermi liquid, a power-law singularity around $k=k_F$,[9]

$$n(k)=n_{kF}-C|k-k_F|^{\alpha}\mathrm{sgn}(k-k_F),\quad n_{kF}=\tfrac{1}{2}\ , \tag{1.1}$$

is expected for the one-dimensional Hubbard model. However, the $g$-ology leading to Eq. (1.1), as well as the quantum Monte Carlo simulation, is essentially based on the analysis of the *weakly correlated regime*. Therefore it is extremely interesting to determine $n(k)$ for the *strongly correlated regime*, which the Bethe-ansatz solution can offer.

The spin correlation function $S(k)$ for the one-dimensional Hubbard model is also of interest for various reasons. First, in the large-$U$ limit at half-filling it is

 

equivalent to what the one-dimensional $S=\frac{1}{2}$ Heisenberg model tells us. When the system is away from half-filling, the spin-correlation function $S(k)$ should be different from that of the Heisenberg model due to the presence of holes. However, the nature of the singularity at $k=2k_F$ has not been clarified yet.[10] Needless to say, the incommensurate spin correlation, which has been observed in $La_{2-x}Sr_xCuO_4$,[11] is also our motivation to study $S(k)$ for the Hubbard model.

Keeping these points in mind, we have studied $n(k)$ and $S(k)$ for the one-dimensional large-$U$ Hubbard model by changing the electron density. In addition to the problems mentioned previously, the present study has revealed a new result, which we had not expected. Namely, a weak singularity is present in $n(k)$ at $k=3k_F$. It is also worth noting here that the momentum of the lowest-energy doped carriers, that was examined in small cluster studies,[12] is closely related to the present study.

This paper is arranged as follows. In Sec. II, we analyze the Bethe-ansatz ground-state wave function in the limit of strong correlation. The momentum distribution as well as the method of calculations will be presented and discussed in Sec. III. In Sec. IV, the spin correlation function $S(k)$ is studied; the peak of $S(k)$ at $2k_F$ is discussed in detail for the quarter-filled band (i.e., $N/N_A=\frac{1}{2}$). We study especially the nature of the $2k_F$ singularity by comparing its size dependence with that of the one-dimensional Heisenberg model. Section V is devoted to a summary and discussions on related problems.

## II. BETHE-ANSATZ WAVE FUNCTION IN THE LARGE-$U$ LIMIT

The one-dimensional Hubbard model is given by

$$H=-t\sum_{(i,j)\sigma}(c_{i\sigma}^{\dagger}c_{j\sigma}+\text{H.c.})+U\sum_i n_{i\uparrow}n_{i\downarrow}\ , \tag{2.1}$$

where $(i,j)$ means the summation over nearest-neighbor pairs. The system consists of $N$ electrons on $N_A$ sites. In this section, we show that the Lieb and Wu wave function[4] for Eq. (2.1) can be reduced to a simple form in the large-$U$ limit. To this end we start by recapitulating the Bethe-ansatz analysis for an arbitrary $U$ and then take the limit of $U/t\rightarrow\infty$.

Let $f(x_1,\ldots,x_N)$ be the amplitude in the wave function when down spins are located at the sites $x_1,\ldots,x_M$, and up spins at $x_{M+1},\ldots,x_N$. Within each region of $x_{Q1}<x_{Q2}<\cdots<x_{QN}$, $f$ is expressed under the Bethe ansatz as

$$f(x_1,\ldots,x_N)=\sum_P[Q,P]\exp\left[i\sum_{j=1}^{N}k_{Pj}x_{Qj}\right]\ , \tag{2.2}$$

where $P=(P1,P2,\ldots,PN)$ and $Q=(Q1,Q2,\ldots,QN)$ are two permutations of $(1,2,\ldots,N)$. The coefficients $[Q,P]$ as well as $(k_1,k_2,\ldots,k_N)$ are determined later. For Eq. (2.2) to satisfy the Schrödinger equation and to be connected properly on each boundary,

$$E=-2t\sum_{j=1}^{N}\cos k_j\ , \tag{2.3}$$

and

$$[Q,P]=Y_{nm}^{i,i+1}[Q,P']\ , \tag{2.4}$$

should hold, where

$$P=(P1,P2,\ldots,Pi=m,P(i+1)=n,\ldots,PN)\ ,$$

and

$$P'=(P1,P2,\ldots,n,m,\ldots,PN)\ .$$

The operator $Y$ is defined by

$$Y_{nm}^{i,i+1}=\frac{P_{i,i+1}-x_{nm}}{1+x_{nm}}\ , \tag{2.5}$$

with

$$x_{nm}=i(U/2)/(t\sin k_n-t\sin k_m)\ ,$$

and $P_{i,i+1}$ is a permutation operator for the interchange between $Qi$ and $Q(i+1)$. Owing to the relation (2.4), we can determine all $[Q,P]$'s from, for example, $[Q,P=\mathbf{1}]$. Here $\mathbf{1}$ means the identity operator.

Eigenvalue equations to determine $k_j$'s are obtained by imposing the periodic boundary condition:

$$e^{ik_jL}[Q,\mathbf{1}]=X_{j+1,j}\cdots X_{Nj}X_{1j}\cdots X_{j-1,j}[Q,\mathbf{1}]\ , \tag{2.6}$$

with

$$X_{ij}=(1-x_{ij}P_{i,j})/(1+x_{ij})\ .$$

It is convenient, however, instead of solving Eq. (2.6), to define

$$\chi(Q)=(-1)^Q[Q,\mathbf{1}]\ , \tag{2.7}$$

and solve the eigenvalue problem

$$e^{ik_jL}\chi(Q)=X'_{j+1,j}\cdots X'_{Nj}X'_{1j}\cdots X'_{j-1,j}\chi(Q)\ , \tag{2.8}$$

with

$$X'_{ij}=(1+x_{ij}P_{i,j})/(1+x_{ij})\ .$$

Here $(-1)^Q$ is equal to $-1$ when $Q$ is an odd permutation and 1 otherwise.

As we can see from the definition of $\chi(Q)$, the antisymmetric property of the wave function is satisfied when $\chi$ has ${}_NC_M$ components of the spin wave function, each of which is characterized by the "coordinates" of $M$ down spins $(y_1,y_2,\ldots,y_M)$ in the spin configuration. For $y_1<y_2<\cdots<y_M$, the eigenvalue problem (2.8) has been solved by Yang[4] with a generalized Bethe's hypothesis as

$$\chi=\Phi(y_1,\ldots,y_M)$$
$$=\sum_P A_PF(\Lambda_{P1},y_1)F(\Lambda_{P2},y_2)\cdots F(\Lambda_{PM},y_M)\ , \tag{2.9}$$

with

$$F(\Lambda,y)=\prod_{j=1}^{y-1}\frac{it\sin k_j-i\Lambda-U/4}{it\sin k_{j+1}-i\Lambda+U/4}\ ,$$
$$A_P=(-1)^P\prod_{i<j}\left[\Lambda_{Pi}-\Lambda_{Pj}-\frac{iU}{2}\right]\ , \tag{2.10}$$

$$-\prod_j\frac{it\sin k_j-i\Lambda_\alpha-U/4}{it\sin k_j-i\Lambda_\alpha+U/4}=\prod_\beta\frac{-i\Lambda_\beta+i\Lambda_\alpha+U/2}{-i\Lambda_\beta+i\Lambda_\alpha-U/2}\ , \tag{2.11}$$

$$e^{ik_jL}=\prod_\beta\frac{it\sin k_j-i\Lambda_\beta-U/4}{it\sin k_j-i\Lambda_\beta+U/4}\ . \tag{2.12}$$

Here $\Lambda_1,\Lambda_2,\ldots,\Lambda_M$ are a set of unequal numbers, which are related to $k_j$'s in a complex manner through Eq. (2.11).

So far no assumption has been made on the magnitude of $U$. A great simplification can be achieved by taking the limit of $U/t\to\infty$. In fact, terms containing $k_j$'s in Eqs. (2.10)–(2.12) can be neglected in the order of $(t/U)^0$ so that $\Lambda_\alpha$'s and $k_j$'s are completely decoupled. In this limit, the operator $Y$ in Eq. (2.5) becomes $-1$, and thus Eq. (2.4) is simply

$$[Q,P]=(-1)^P[Q,\mathbf{1}]\ . \tag{2.13}$$

Therefore, combining Eqs. (2.2), (2.7), and (2.9), we obtain

$$f(x_1,\ldots,x_N)=\sum_P(-1)^P(-1)^Q\Phi(y_1,\ldots,y_M)\exp\left[i\sum_{j=1}^N k_{Pj}x_{Qj}\right]$$
$$=(-1)^Q\det[\exp(ik_ix_{Qj})]\Phi(y_1,\ldots,y_M)\ . \tag{2.14}$$

The determinant depends only on the sites of particles $(x_{Q1}<\cdots<x_{QN})$ and not on their spins. Thus it is the same as the Slater determinant of spinless fermions with momenta $k_j$'s. This means a decoupling between the charge and spin degrees of freedom for $U/t\to\infty$.

Furthermore, we can show that $\Phi(y_1,\ldots,y_M)$ in this limit is just the same as the Bethe's exact solution of the one-dimensional Heisenberg spin system. To do this explicitly, we introduce from $\Lambda_\alpha$'s new quantities $f_\alpha(0\le f_\alpha<2\pi)$ and $\phi_{\alpha\beta}(-\pi\le\phi_{\alpha\beta}<\pi)$ by

$$\theta(2\Lambda_\alpha)=\pi-f_\alpha\ ,$$
$$\theta(\Lambda_\alpha-\Lambda_\beta)=\pi-\phi_{\alpha\beta}\ \ (\mathrm{mod}2\pi)\ , \tag{2.15}$$

where $\theta(p)=-2\tan^{-1}(2p/U)$. By taking account of the branch of $\tan^{-1}$ which shows up in the definition of $\phi_{\alpha\beta}$, we can rewrite Eq. (2.10) as

$$F(\Lambda_\alpha,y)=\exp[i(y-1)f_\alpha]$$

and

$$A_P=\exp\left[(i/2)\sum_{k<l}(\phi_{Pk,Pl}-\pi)\right]\ .$$

Then the spin wave function becomes

$$\Phi(y_1,\ldots,y_M)=\sum_P\exp\left[i\sum_{k=1}^M f_{Pk}y_k+\frac{i}{2}\sum_{k<l}\phi_{Pk,Pl}\right], \tag{2.16}$$

except for a constant phase factor. Equation (2.16) corresponds exactly to the Bethe-ansatz wave function for the one-dimensional Heisenberg model.[6] The relation between $\phi_{\alpha\beta}$ and $f_\alpha$ is obtained from Eq. (2.11) as

$$\cot\left[\frac{\phi_{\alpha\beta}}{2}\right]=\frac{1}{2}\left[\cot\frac{f_\alpha}{2}-\cot\frac{f_\beta}{2}\right]\ , \tag{2.17}$$

which is nothing but an expression for the scattering phase shift in the Bethe's solution.

Finally we need the momenta $k_j$'s to obtain the explicit form of the wave function in Eq. (2.14). In the large-$U$ limit, Eqs. (2.11) and (2.12) lead to

$$k_jL=2\pi I_j-\sum_\beta\theta(2\Lambda_\beta)$$
$$=2\pi\left[I_j+\frac{1}{N}\sum_\alpha J_\alpha\right]\ , \tag{2.18}$$

with

$$I_j=\begin{cases}\text{integer} & \text{for } M \text{ even}\ ,\\ \text{half-odd integer} & \text{for } M \text{ odd}\ ,\end{cases} \tag{2.19}$$

$$J_\alpha=\begin{cases}\text{integer} & \text{for } N-M=\text{odd}\ ,\\ \text{half-odd integer} & \text{for } N-M=\text{even}\ .\end{cases}$$

For example, in the case of $N=$even and $M=$odd, the ground state corresponds to

$$I_j=\left\{-\frac{N-1}{2},-\frac{N-3}{2},\ldots,-\frac{1}{2},\frac{1}{2},\ldots,\frac{N-1}{2}\right\}, \tag{2.20}$$

$$J_\alpha=\left\{-\frac{M-1}{2},-\frac{M-3}{2},\ldots,-1,0,1,\ldots,\frac{M-1}{2}\right\}.$$

In this case, $k_j$'s are just the same as the momenta of spinless fermions under the *antiperiodic* boundary condition. This gives the lowest energy of $U=\infty$.

Before closing this section several remarks are in order.

(1) We note that all the spin configurations become degenerate at $U=\infty$. Our wave function in Eq. (2.14) has been derived by taking the limit of $U/t\to\infty$. Therefore

it represents for the ground state a singlet wave function which is connected naturally to the ground state in the whole region of $0<U<\infty$. In other words, the degeneracy at $U=\infty$ is removed by an infinitesimal perturbation of the order $t/U$. This is the reason why the Heisenberg-type spin wave function shows up. As demonstrated explicitly in Appendix A, the wave function of Eq. (2.14) gives the correct ground-state energy up to the order of $t/U$.

(2) Our wave function is naturally related to the half-filled case where it is well known that the Hubbard model is transformed into the $S=\frac{1}{2}$ Heisenberg model.

(3) There is a subtle problem in a system with $N=4n$ electrons, with $n$ being an integer. In fact, we can see that the ground state in this case is a triplet if the periodic boundary condition is applied. For the singlet lowest-energy wave function, we have $N=$even and $M=N/2=$even so that

$$I_j=\left\{-\frac{N}{2},-\frac{N}{2}+1,\ldots,-1,0,1,\ldots,\frac{N}{2}-1\right\}, \tag{2.21}$$

$$J_\alpha=\left\{-\frac{M-1}{2},-\frac{M-3}{2},\ldots,-\frac{1}{2},\frac{1}{2},\ldots,\frac{M-1}{2}\right\}.$$

In this case, the momenta $k_j$ determined from (2.18) are the same as those for spinless fermions under the *periodic* boundary condition. On the other hand, for the triplet ($S=1$) lowest-energy wave function ($N=$even and $M=N/2+1=$odd), $I_j$ and $J_\alpha$ are given by Eq. (2.20), and thus $k_j$'s are the same as the momenta for spinless fermions under the *antiperiodic* boundary condition. Comparing the energy $E=-2t\sum_j \cos k_j$ for both cases, we find that the triplet state has a lower energy. We have confirmed this also by an exact diagonalization of the eight-site Hubbard chain.

To study singlet ground-state wave functions also for the systems with $4n$ electrons which are lower than the triplet ones, we use the antiperiodic boundary condition for this case instead of the periodic one. For the antiperiodic boundary condition, we only have to change the left-hand side of the eigenvalue problem (2.8) as

$$-e^{ik_jL}\chi(Q)\ . \tag{2.22}$$

This change leads to an alternative relation

$$I_j=\begin{cases}\text{half-odd integer} & \text{for } M \text{ even}\ ,\\ \text{integer} & \text{for } M \text{ odd}\ ,\end{cases} \tag{2.23}$$

which guarantees that the singlet lowest-energy wave function ($M=N/2=$even) becomes the ground state, because the momenta $k_j=2\pi I_j/L$ are those for spinless fermions under the antiperiodic boundary condition. In the following sections, therefore, we study two cases, (i) $N=4n+2$ with the periodic boundary condition and (ii) $N=4n$ with the antiperiodic boundary condition. For these cases, the ground state is always a singlet and the total momentum is equal to zero.

(4) One may wonder why Eq. (2.2) is not enough to evaluate physical quantities. The reason is that, because of the permutation, Eq. (2.2) is extremely complicated and useless for practical calculations: with Eq. (2.2) one cannot go beyond the system size for which the exact diagonalization method is applicable. On the other hand, Eq. (2.14) is much simpler, as will be discussed further in the next section.

## III. MOMENTUM DISTRIBUTION FUNCTION

In the preceding section, we have obtained the ground-state wave function, which is simple due to a decoupling between charge and spin degrees of freedom. This simplicity enables us to study relatively large systems, whose wave functions are almost impossible to handle otherwise.

In practice we construct the ground-state wave function as follows.

(1) First, we determine $\Phi(y_1,\ldots,y_M)$ by diagonalizing the one-dimensional Heisenberg model. In this way the ground state up to 26 spins can be obtained by using the Lanczos method and conjugate gradient method.[12,13] The $z$ component of the total spin and the total momentum are used to classify the states.

(2) Next, we calculate the Slater determinant describing the charge degrees of freedom, making use of the Vandermonde determinant.[14] In the one-dimensional system, each matrix element has the form

$$\exp(ik_lr_m)\ , \tag{3.1}$$

with

$$k_l=k_0+(l-1)\Delta k\quad (l=1,\ldots,N)\ . \tag{3.2}$$

In our case, where $k_0=-(N-1)\pi/L$ and $\Delta k=2\pi/L$, the determinant is simply expressed as

$$\det[\exp(ik_lr_m)]=\prod_{l<m}\left[2i\sin\frac{\Delta k(r_l-r_m)}{2}\right]. \tag{3.3}$$

This formula reduces computational time drastically.[14] The maximum size we treat here is 16 fermions on 32 sites, for which the number of configurations of spinless fermions is ${}_{32}C_{16}=601\,080\,390$.

To determine the momentum distribution $n(k)$, we go back to its definition in real space:

$$n(k)=\langle c_{k\sigma}^\dagger c_{k\sigma}\rangle=\frac{1}{N_A}\sum_{jl}\langle c_{j\sigma}^\dagger c_{l\sigma}\rangle e^{ik(r_j-r_l)}\ . \tag{3.4}$$

The average $\langle\ \rangle$ is taken over the ground-state wave function (2.14). When an electron with spin $\sigma$ is transferred from the $l$th site to the $j$th site as in the right-hand side of Eq. (3.4), the spin configuration is changed in general (see Fig. 1). Therefore $\langle c_{j\sigma}^\dagger c_{l\sigma}\rangle$ can be written as

$$\langle c^{\dagger}_{j\sigma}c_{l\sigma}\rangle = \sum_{\text{configurations of spinless fermions}} (-1)^{Q-Q'}(\mathcal{S})^{*}(\mathcal{S})'\omega(l\rightarrow j,\sigma)\ , \tag{3.5}$$

where $(\mathcal{S})$ denotes the Slater determinant of Eq. (2.14) and $(\mathcal{S})'$ is the same wave function except that a fermion on the $l$th site has been moved onto the $j$th site. $\omega(l\rightarrow j,\sigma)$ contains the sum over all the spin configurations and takes account of the change in $\Phi(y_1,\ldots,y_M)$ by this transfer:

$$\begin{aligned}&\omega(l\rightarrow j,\sigma)=\omega_{l'\rightarrow j'}/2\ ,\\ &\omega_{l'\rightarrow j'}\equiv\langle(2\mathbf{S}_{j'}\cdot\mathbf{S}_{j'-1}+\tfrac{1}{2})(2\mathbf{S}_{j'-1}\cdot\mathbf{S}_{j'-2}+\tfrac{1}{2})\cdots(2\mathbf{S}_{l'+1}\cdot\mathbf{S}_{l'}+\tfrac{1}{2})\rangle_H\ ,\end{aligned} \tag{3.6}$$

where the $l'$th spin corresponding to the electron on the $l$th site jumps over some other spins to become the $j'$th spin corresponding to the electron on the $j$th site due to the operation of $c^{\dagger}_{j\sigma}c_{l\sigma}$. $(2\mathbf{S}_{j'}\cdot\mathbf{S}_{j'-1}+\frac{1}{2})$ takes care of the exchange between the $j'$th and $(j'-1)$th spins, and $\langle\ \rangle_H$ denotes the expectation value over the ground state of the Heisenberg model. Using this expression (3.5), we actually carried out the calculation through two steps. First, $\omega(l\rightarrow j,\sigma)=\omega_{l'\rightarrow j'}/2$ was evaluated by fixing the configuration of spinless fermions; then the summation over all the configurations was performed with Eq. (3.5).

Before showing the results, it is useful to note a feature of the momentum distribution. Since the wave function contains the Slater determinant of spinless fermions, one may think that $n(k)$ must have a jump at $k=2k_F$. This is not the case, however, because of $\omega(l\rightarrow j,\sigma)$. In the pure spinless fermion case, the factor $\omega(l\rightarrow j,\sigma)$ is unity, so that Eq. (3.5) is just a difference in the Slater determinant induced by the change of the configurations. In our case, on the other hand, the spin degrees of freedom $\Phi(y_1,\ldots,y_M)$ are also changed when an electron is transferred from the $l$th site to the $j$th site. This change in $\Phi$ shows up in $\omega(l\rightarrow j,\sigma)$ and leads to an essential difference from the spinless fermion case. In Fig. 2, we show $\omega_{l'\rightarrow j'}$ for a chain of 26 spins as a function of $|j'-l'|$. Clearly $\omega_{l'\rightarrow j'}$ has an oscillatory behavior like

$$\omega_{l'\rightarrow j'}\sim\cos\left[\frac{\pi}{2}|j'-l'|+\frac{\pi}{4}\right]\ , \tag{3.7}$$

for large $|j'-l'|$. This oscillation smears out the $2k_F$ singularity in the spinless fermion wave function.

We now present the results of the momentum distribution in Fig. 3. As a typical case, the quarter-filled system (i.e., $N/N_A=\frac{1}{2}$) is chosen here and the size dependence is studied systematically. As mentioned in the preceding section, we take the periodic boundary condition for $N=6,10,14$ systems and the antiperiodic one for $N=4,8,12,16$ systems. These results combined together nicely tell us the $k$ dependence of $n(k)$ for the infinite system, except for $k\sim k_F$ and $k\sim 3k_F$. It is readily seen that there is no detectable singularity at $k=2k_F$. Instead, one notices a strong singularity at $k_F$ and a weak singularity at $k=3k_F$. In order to confirm that the latter is really associated with $3k_F$, we have studied a different system with the electron density of $\frac{14}{30}$. As shown in Fig. 4, the singularity assigned as $3k_F$ has shifted in accordance with the expectation. Figure 5 presents a systematic change of the dependence of $n(k)$ on the filling factor. There exist always noticeable singularities at $k_F$ and $3k_F$. Note that, when $3k_F$ becomes larger than $\pi$, it is folded back into the Brillouin zone and appears at $2\pi-3k_F$. This also explains the nonmonotonic $k$ dependence of $n(k)$ for the electron density close to half-filling, i.e., $\frac{20}{28}-\frac{26}{28}$.

Let us investigate the singularity at $k=k_F$ in more detail. In Table I, $n(k)$ in the vicinity of $k_F$ for the

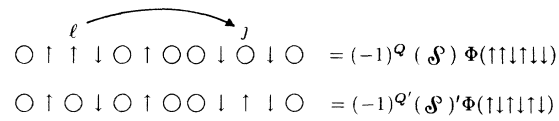


FIG. 1. A schematic picture of the effect of $c^{\dagger}_{j\sigma}c_{l\sigma}$ on the wave function. The upper part represents a certain configuration $|i\rangle$ in the ground-state wave function, whose amplitude $f(x_1,\ldots,x_N)$ is indicated on the right-hand side. The lower part represents the configuration after an electron is transferred from the $l$th site to the $j$th site, i.e., $c^{\dagger}_{j\sigma}c_{l\sigma}|i\rangle$. Note that the spin wave function $\Phi$ changes as well as the Slater determinant.

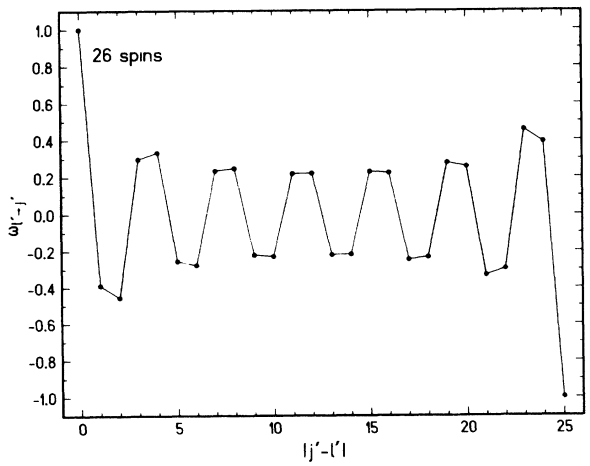


FIG. 2. "Spin transfer" $\omega_{l'\rightarrow j'}$ as a function of $|j'-l'|$ evaluated for a chain of 26 spins. As defined in Eq. (3.6), it represents the expectation value when the $l'$th spin jumps over some other spins to become the $j'$th spin. This quantity appears in the calculation of $\langle c^{\dagger}_{j\sigma}c_{l\sigma}\rangle$ to take account of the change in the spin wave function induced by the operation $c^{\dagger}_{j\sigma}c_{l\sigma}$. Note that $\omega_{l'\rightarrow j'}=1$ when $l'$ is equal to $j'$, because the spin configuration does not change in this case. For $j'-l'=N-1=25$, the spin configuration shifts by the unit lattice constant and thus $\omega_{l'\rightarrow j'}=(-1)^{N/2}=-1$.

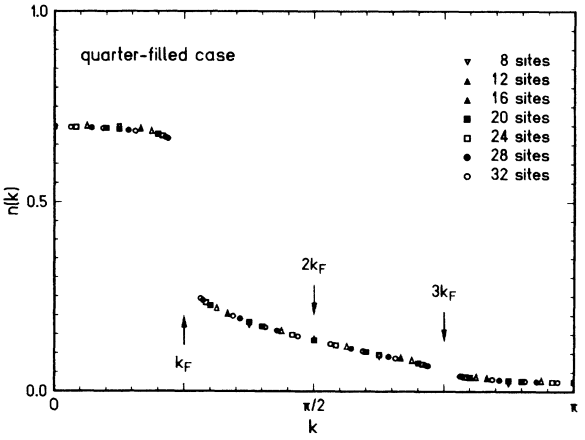


FIG. 3. The momentum distribution $n(k)$ for the quarter-filled case when $U/t \to \infty$. The periodic boundary condition is assumed for $N_A = 12$, 20, and 28 (solid symbols), while the antiperiodic one is taken for $N_A = 8$, 16, 24, and 32 (open symbols). $k_F$, $2k_F$, and $3k_F$ are indicated by arrows.

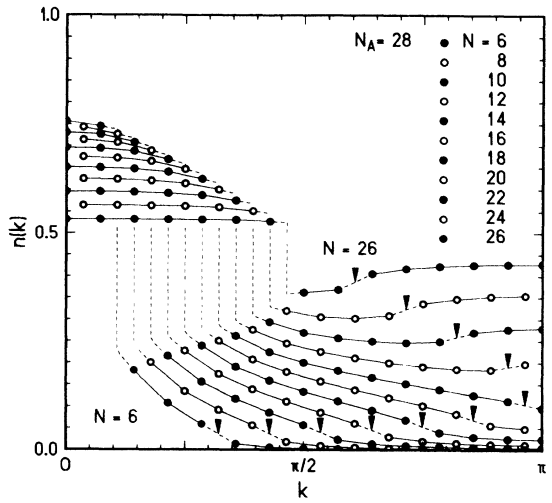


FIG. 5. The momentum distribution $n(k)$ for systems with various electron numbers $N = 6$–$26$ with $N_A$ fixed at 28. Since the nature of the singularities has not been determined precisely, dashed lines are drawn around $k_F$ and $3k_F$ as guides to the eyes. Otherwise, the data points are connected by solid lines for convenience. $3k_F$ is indicated by an arrow for each electron density. Note that, for $N \geq 20$, $3k_F$ becomes larger than $\pi$ and appears at $2\pi - 3k_F$.

quarter-filled case is summarized. Having the formula (1.1) in mind, we plot in Fig. 6

$$\ln|n(k) - n_{kF}| - \ln|n(k_0) - n_{kF}|$$

as a function of $\ln|k - k_F| - \ln|k_0 - k_F|$ for $n_{kF} = 0.4 \sim 0.6$. Here $k_0$ is the momentum that is the closest to $k_F$, i.e., $|k_0 - k_F| = \pi/32$ in our calculation. First, we analyze the data by taking $n_{kF} = \frac{1}{2}$ as in the $g$-ology. From the slope of two points closest to $k_F$, we obtain $\alpha = 0.136$ for $k < k_F$ and $\alpha = 0.147$ for $k > k_F$. It is evident from Fig. 6 that if we had larger systems, we would have $\alpha > 0.136$ for $k < k_F$ and $\alpha < 0.147$ for $k > k_F$. Physically it is natural to expect the value of $\alpha$ to be the same for both $k < k_F$ and $k > k_F$. Therefore we conclude that $0.136 < \alpha < 0.147$, i.e., $\alpha \simeq 0.14$.

Next, we try to change $n_{kF}$ from $\frac{1}{2}$ regarding it as a fitting parameter. When $n_{kF} > 0.5$ is assumed, it is impossible to obtain an $\alpha$ that is the same for both $k < k_F$ and $k > k_F$, because the two inequalities for $\alpha$ derived from the size dependence in Fig. 6 are not compatible. In fact, we find that even for $n_{kF} > 0.507$, there is no region for $\alpha$ satisfying the two inequalities. On the other hand, when $n_{kF} < 0.5$ is taken, the difference between the upper bound and the lower bound for $\alpha$ becomes large. In this case it seems difficult to expect that $\alpha$ converges to a common value for $k < k_F$ and $k > k_F$ in the larger systems. Thus it is very likely that $n(k)$ has a power-law

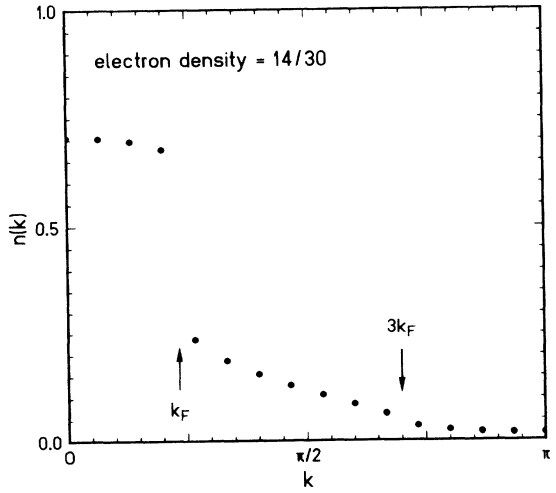


FIG. 4. The momentum distribution $n(k)$ for the system with $N/N_A = \frac{14}{30}$. Note a weak singularity at $k = 3k_F$ in accordance with the expectation.

TABLE I. The momentum distribution $n(k)$ in the vicinity of $k_F$ for the quarter-filled case.

| $N_A$ | $k/\pi$ | $n(k)$ $(k < k_F)$ | $k/\pi$ | $n(k)$ $(k > k_F)$ |
|---|---|---|---|---|
| 8 | $\frac{1}{8}$ | 0.699 706 6 | $\frac{3}{8}$ | 0.177 906 9 |
| 12 | $\frac{2}{12}$ | 0.689 296 4 | $\frac{4}{12}$ | 0.200 914 9 |
| 16 | $\frac{3}{16}$ | 0.682 407 7 | $\frac{5}{16}$ | 0.215 093 9 |
| 20 | $\frac{2}{20}$ | 0.693 272 5 | $\frac{6}{20}$ | 0.225 120 7 |
| | $\frac{4}{20}$ | 0.677 181 5 | $\frac{8}{20}$ | 0.170 033 0 |
| 24 | $\frac{3}{24}$ | 0.690 412 4 | $\frac{7}{24}$ | 0.232 767 6 |
| | $\frac{5}{24}$ | 0.672 958 7 | $\frac{9}{24}$ | 0.181 360 9 |
| 28 | $\frac{4}{28}$ | 0.687 776 2 | $\frac{8}{28}$ | 0.238 888 3 |
| | $\frac{6}{28}$ | 0.669 415 1 | $\frac{10}{28}$ | 0.190 315 6 |
| 32 | $\frac{5}{32}$ | 0.685 362 8 | $\frac{9}{32}$ | 0.243 955 4 |
| | $\frac{7}{32}$ | 0.666 364 1 | $\frac{11}{32}$ | 0.197 656 0 |

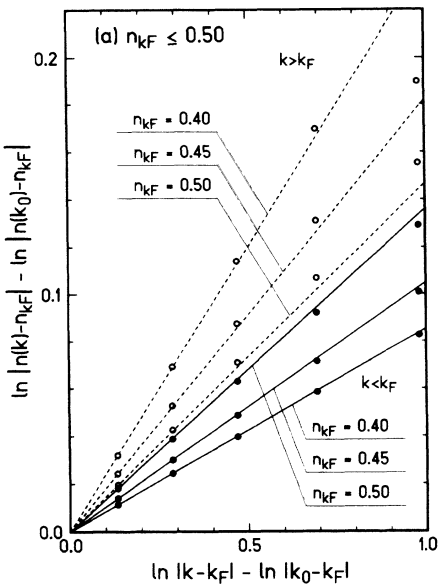


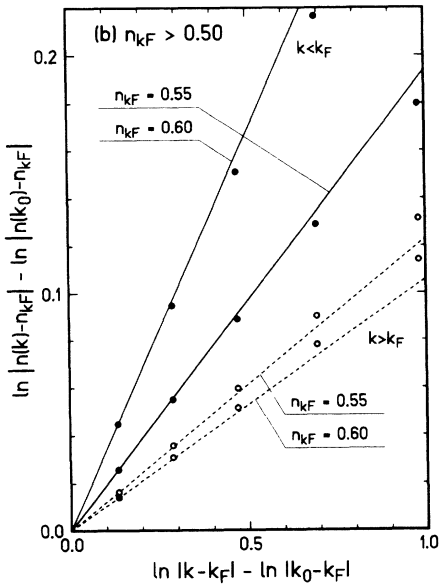


FIG. 6. The momentum distribution $|n(k)-n_{kF}|$ near $k_F$ as a function of $|k-k_F|$ for the quarter-filled case. Several values are assumed for $n_{kF}$: (a) $n_{kF} \le 0.50$ and (b) $n_{kF} > 0.50$. The value of $n(k)$ is plotted whose momentum $k$ is the nearest to $k_F$, i.e., $|k-k_F| = \pi/N_A$ for each $N_A$ site system. Solid (open) circles represent $n(k)$ just below (above) $k_F$. Note that $n(k)$ has a smooth $k$ dependence even though the results for periodic and antiperiodic boundary conditions are shown together. The origin is chosen to be the point for the largest size ($N_A = 32$) whose momentum $k_0$ is the closest to $k_F$. The solid (dashed) lines connect two points nearest to $k_F$ below (above) $k_F$; thus their gradients represent the exponent $\alpha$'s discussed in the text.

singularity at $k_F$ with $n_{kF} = \frac{1}{2}$ just as the $g$-ology predicts for the weak-coupling region.

Although the present work is featured by studies of the strong-correlation regime, the relation to the weak-correlation regime is also of interest. In Appendix B, we summarize the second-order perturbation calculation of $n(k)$. The second-order correction to $n(k)$, which is divergent at $k = k_F$ as $\ln|k-k_F|$, is shown explicitly. This divergence smears out the jump at $k = k_F$ even when an infinitesimal $U$ is present, and $n(k)$ naturally comes to have the power-law dependence as in Eq. (1.1). These arguments are restricted in the weak-coupling regime. However, since there is no phase transition in the finite $U$ region, we think that a formula similar to Eq. (1.1) will hold even in the large-$U$ limit.

This perturbation calculation presented in Appendix B also shows a weak singularity at $3k_F$. According to our results, the singularity at $3k_F$ is weak even in the limit of $U/t \to \infty$, so that we will not go into an analysis of the exact nature of the singularity. However, from the result of the perturbation calculation in Appendix B and from Fig. 3, we speculate $n(k)$ to have a cusplike singularity at $3k_F$.

Finally we examine a case close to half-filling, since a recent Monte Carlo simulation[8] has reported that the singularity of $n(k)$ near $k_F$ is smeared out at least in the two-dimensional Hubbard model. Figure 7 shows our result for the electron density of $\frac{26}{32}$. This result is qualitatively similar to that for lower electron densities shown in Fig. 5. The $3k_F$ singularity also shows up at $k = 2\pi - 3k_F = 0.78\pi$. It would be interesting to see what the Monte Carlo simulation[8,15] predicts for the strong-correlation regime.

## IV. SPIN-CORRELATION FUNCTION

The Fourier transform of the spin-correlation function is defined by

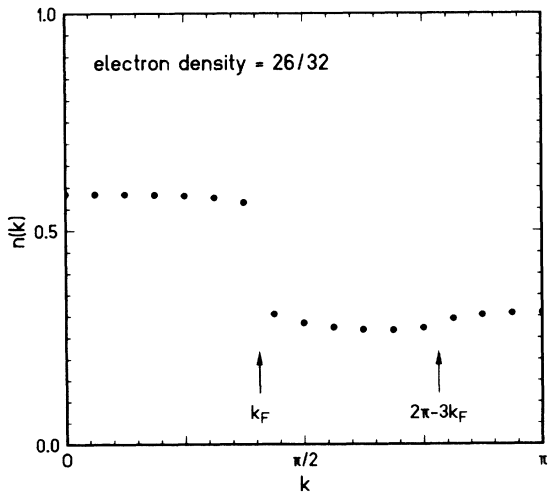


FIG. 7. The momentum distribution $n(k)$ for the system with $N/N_A = \frac{26}{32}$, which is close to half-filling. The $3k_F$ singularity shows up at $k = 2\pi - 3k_F = 0.78\pi$.

$$S(k)=\frac{1}{N_A}\sum_{j,l}\langle S_j^z S_l^z\rangle e^{ik(r_j-r_l)} . \quad (4.1)$$

Although the spin degrees of freedom in the ground state of $U/t\to\infty$ are completely described by that of the Heisenberg model, the spin-correlation function for less-than-half-filled systems is, of course, different. The reason is simply that $\langle S_j^z S_l^z\rangle$ is not identical to $\langle S_j^z S_l^z\rangle_H$ in the Heisenberg model because of the presence of holes: $|j-l|$ is, in general, different from the distance in the Heisenberg model.

As in the case of $n(k)$, we can write $\langle S_j^z S_l^z\rangle$ in Eq. (4.1) as

$$\langle S_j^z S_l^z\rangle=\sum_{\text{configurations of spinless fermions}}|\mathcal{S}|^2\langle S_{j'}^z S_{l'}^z\rangle_H , \quad (4.2)$$

where $j'$ and $l'$ are related to $j$ and $l$ in the same way as explained after Eq. (3.6). Equation (4.2) has been used to evaluate $S(k)$ for various electron densities, examples of which are presented in Fig. 8 with $S_H(k)$ in the Heisenberg model. Clearly a peak shows up at $k=2k_F$, which is incommensurate when the system is away from half-filling. It is much enhanced from a cusp for $U=0$, that is shown for a comparison. As discussed in Appendix B, in the weak correlation regime the perturbation theory predicts that the first-order correction to $S(k)$ already contains a stronger singularity, which naturally explains a peak of $S(k)$ at $k=2k_F$. Our result for $U/t\to\infty$ shown in Fig. 8 should be compared with this weak-correlation behavior. One also notices that the enhancement of $S(k)$ becomes weaker as the system deviates from half-filling. It is consistent with the dependence on the electron density of the perturbation theory discussed in Appendix B.

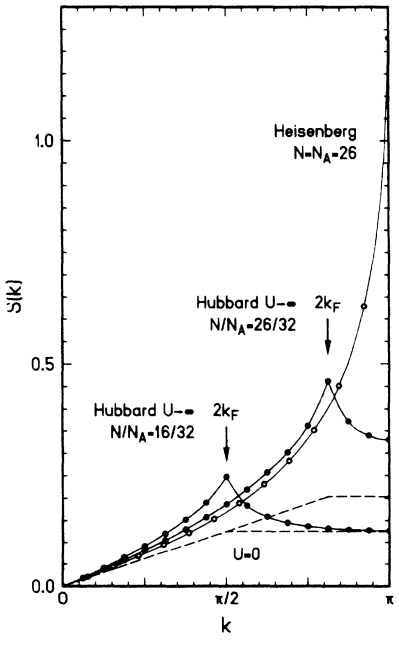


FIG. 8. The spin correlation functions $S(k)$ for the systems with $N/N_A=\frac{26}{32}$ and $\frac{16}{32}$ when $U/t\to\infty$. $S(k)$ for $U=0$ with the same electron densities (dashed lines) and $S_H(k)$ for the 26-site Heisenberg model (open circles) are also depicted. For each system, $2k_F$ is indicated by an arrow.

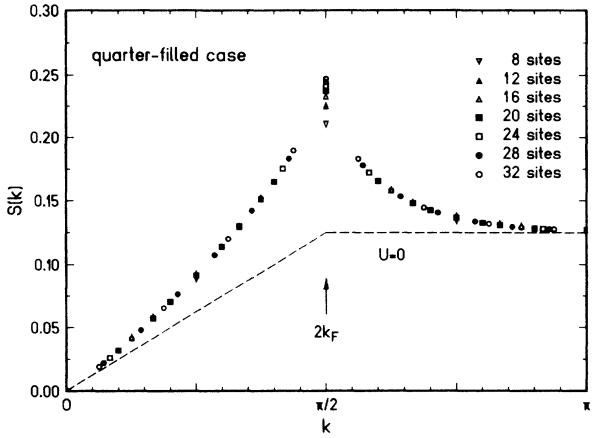


FIG. 9. The spin correlation function for $U/t\to\infty$ in the quarter-filled case. $N_A=12$, 20, and 28 site systems are under the periodic boundary condition (solid symbols), while $N_A=8$, 16, 24, and 32 are under the antiperiodic boundary condition (open symbols). $2k_F=\pi/2$ is indicated by an arrow. For a comparison, the results for $U=0$ are also shown by a dashed line.

To examine the singularity at $2k_F$ in more detail, we have studied $S(k)$ for various system sizes by fixing the electron density at the quarter-filled case (i.e., $N/N_A=\frac{1}{2}$). It is readily seen from Fig. 9 that the size dependence is evident especially at $k=2k_F=\pi/2$, suggesting convincingly a singularity at this point.

Although Monte Carlo simulations[10] have found this $2k_F$ peak, its size dependence has not been studied systematically. The peak $S(2k_F)$ we have obtained is shown in Table II. It is plotted as a function of the system size $N_A(=2N)$ in Fig. 10. For a comparison, we have also calculated and plotted the peak $S_H(\pi)$ in the Heisenberg model. Clearly the peak $S(2k_F)$ for the large-$U$ Hubbard model is drastically reduced compared to $S_H(\pi)$ in the

TABLE II. The size dependence of $S(2k_F)$ for the quarter-filled case in the $U/t\to\infty$ Hubbard model ($N_A=2N$), and that of $S_H(\pi)$ for the Heisenberg model ($N_A=N$).

| $N_A$ | $S(2k_F)$ | $S_H(\pi)$ |
|---|---|---|
| 4 | | 0.666 666 7 |
| 6 | | 0.777 350 1 |
| 8 | 0.211 531 0 | 0.860 452 7 |
| 10 | | 0.927 133 3 |
| 12 | 0.223 824 4 | 0.982 908 6 |
| 14 | | 1.030 907 5 |
| 16 | 0.231 591 3 | 1.073 075 9 |
| 18 | | 1.110 707 1 |
| 20 | 0.237 066 3 | 1.144 704 7 |
| 22 | | 1.175 725 1 |
| 24 | 0.241 194 3 | 1.204 260 5 |
| 26 | | 1.230 689 3 |
| 28 | 0.244 452 0 | |
| 30 | | |
| 32 | 0.247 109 1 | |

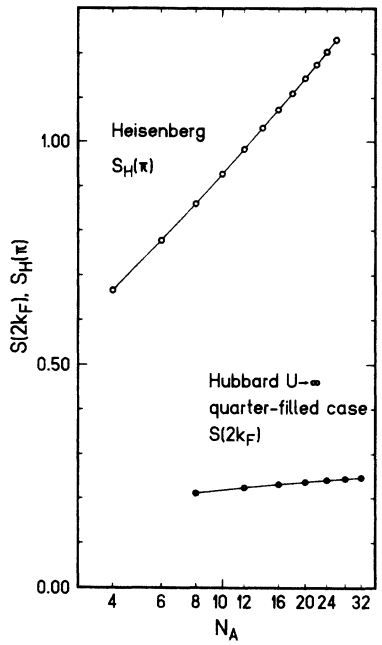


FIG. 10. The system size dependence of the peak $S(2k_F)$ for the quarter-filled case. The same quantity for the Heisenberg model, $S_H(\pi)$, is also shown by open circles for a comparison. Notice that $S(2k_F)$ has a weaker size dependence than $\ln N_A$ and that its absolute value is drastically reduced from the Heisenberg case.

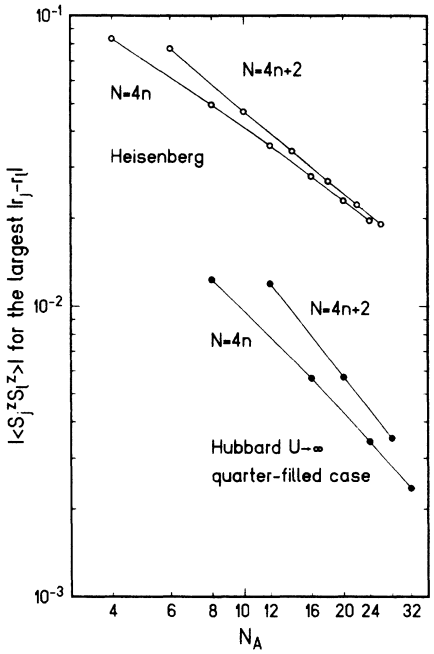


FIG. 11. The spin correlation $\langle S_j^z S_l^z \rangle$ with the largest $|r_j - r_l|$ is plotted in a log-log scale by taking the quarter-filled case. Open circles represent the same quantity in the Heisenberg model, which is shown for a comparison. Note that there are two series in the size dependence: the systems with $N = N_A/2 = 4n$ and $N = 4n + 2$.

Heisenberg model. This is due to the presence of holes moving in the system. Furthermore, we can see that the peak $S(2k_F)$ has a weaker size dependence than $\ln N_A$, while $S_H(\pi)$ has a stronger size dependence than $\ln N_A$. In the latter case, Kubo *et al.*[16] have extensively studied and concluded that

$$\langle S_j^z S_l^z \rangle_H \sim \frac{1}{|r_j - r_l|} \left[ \ln \left| \frac{r_j - r_l}{r_0} \right| \right]^{\sigma} \cos[\pi(r_j - r_l)] , \tag{4.3}$$

holds for large $|r_j - r_l|$ with $0.2 < \sigma < 0.3$, and hence $S_H(\pi)$ has a size dependence as

$$S_H(\pi) \sim \left[ \ln \left[ \frac{N_A}{2r_0} \right] \right]^{1+\sigma} . \tag{4.4}$$

It is consistent with the results in Fig. 10.

The size dependence of $S(2k_F)$ in the less-than-half-filled case, which is weaker than that in the Heisenberg model, indicates that $\langle S_j^z S_l^z \rangle$ decays faster than $1/|r_j - r_l|$. In Fig. 11, we plot the value of $\langle S_j^z S_l^z \rangle$ for the largest $(r_j - r_l)$ in a log-log scale. For a comparison, a similar plot is also made for the Heisenberg model. Fitting two points for the largest sizes with a formula

$$\langle S_j^z S_j^l \rangle \sim |r_j - r_l|^{-\eta} , \tag{4.5}$$

we obtain $\eta = 1.44$ for the systems under the periodic boundary condition ($N_A = 20, 28$) and $\eta = 1.29$ for the systems under the antiperiodic boundary condition ($N_A = 24, 32$). As is evident from Fig. 11, we would have $1.29 < \eta < 1.44$ if we could study larger systems. On the other hand, a similar estimation for the Heisenberg model gives $\eta = 0.933$ from the two points for $N_A = 22$ and 26 and $\eta = 0.877$ from $N_A = 20$ and 24, which are different from Eq. (4.3). Clearly larger systems have to be studied to detect a possible existence of a logarithmic factor in Eq. (4.5). That is beyond the scope of this paper.

The present study showed that the decay of spin correlation in the less-than-half-filled case is different from that in the Heisenberg model. The physical origin of this difference can be understood from the wave function (2.14). Since the number of fermions present between $r_j$ and $r_l$ varies, the summation in Eq. (4.2) contains $\langle S_{j'}^z S_{l'}^z \rangle_H$ for various $(r_{j'} - r_{l'})$'s. Owing to the oscillatory behavior of $\langle S_{j'}^z S_{l'}^z \rangle_H$, the absolute value of $\langle S_j^z S_l^z \rangle$ is reduced and its decay for large $|r_j - r_l|$ should become faster.

## V. SUMMARY AND DISCUSSION

In this paper we have studied the momentum distribution and spin-correlation functions in the large-$U$ limit of the one-dimensional Hubbard model. It is based on the Bethe-ansatz wave function of finite, but fairly large systems. To our knowledge, this is the first attempt to calculate physical quantities by using the Bethe-ansatz wave function. Let us summarize our main results and discuss related problems.

(1) Generally, the propagation of electrons in strongly correlated systems is greatly affected by rearrangements

of surrounding spins.[12,17] In the large-$U$ limit of the one-dimensional Hubbard model, this interplay shows up in a simple way. Namely, the ground-state wave function can be expressed as a product of a Slater determinant of spinless fermions and the spin wave function of the one-dimensional $S=\frac{1}{2}$ Heisenberg model. The rearrangement of spin configuration plays an essential role in $n(k)$ through the "spin transfer" $\omega_{l'\to j'}$, which is an oscillatory function of the distance and smears out the singularity of $n(k)$ at $k=2k_F$ of spinless fermions and leads to a strong singularity at $k_F$.

(2) Since our calculation has been carried out for large, but finite systems, it was unfortunately difficult to completely determine the nature of singularity of $n(k)$ at $k=k_F$. However, present results strongly suggest that the power-law singularity as predicted by the $g$-ology [Eq. (1.1)] also applies to this $U/t\to\infty$ case. We have tried to estimate the exponent $\alpha$ from the size dependence for a typical density, i.e., the quarter-filled system, and found that $\alpha$ is as small as 0.13–0.15 even in the large-$U$ limit. In the $g$-ology, $\alpha$ is given by

$$\alpha=\frac{1}{8\pi^2}\frac{g_2^2}{v_F^2}\ , \tag{5.1}$$

where $v_F$ is the Fermi velocity and $g_2$ is equal to $U$ according to the mapping from the Hubbard model to the Tomonaga-Luttinger model. The perturbation calculation in Appendix B also suggests this exponent.[18] In the quarter-filled case, $v_F=\sqrt{2}t$ and thus we have $\alpha=U^2/16\pi^2t^2$. This gives $\alpha=0.1$ already at $U=4t$.

(3) We have found a new singularity of $n(k)$ at $k=3k_F$ or $2\pi-3k_F$. It is due to a pair of electron-hole excitations, as explained in Appendix B. It is natural then to think that a progressively weaker singularity caused by multipairs of electron-hole excitations must be present, in principle, also at $k=5k_F$, $7k_F$, . . . . Presumably they are not detectable in our results because they are very weak and we just have discrete wave numbers due to the finite system size.

(4) The peak of $S(k)$ shows up at $k=2k_F$, which is incommensurate when the system is away from half-filling. The precise nature of the singularity of $S(k)$ at $k=2k_F$ is a subtle problem because a reliable extrapolation to $N_A\to\infty$ is needed. However, we can say that the size dependence of $S(2k_F)$ for the quarter-filled case is weaker than $\ln N_A$, in contrast to the half-filled case corresponding to the Heisenberg model.

(5) Sorella[19] showed that for the weak-correlation regime ($U/t=4$) their Monte Carlo results on $n(k)$ for a finite system can be well described by the perturbation theory. They seem to be consistent also with the prediction of $g$-ology. As for $S(k)$ a peak at $k=2k_F$ is clearly observed in the Hirsch and Scalapino[10] and Imada and Hatsugai[15] Monte Carlo results; however, the nature of the singularity has not been analyzed by them, possibly because of statistical fluctuations inherent in their Monte Carlo procedure. A refinement of statistics as well as an extension to the strong-correlation regime would be extremely important in the Monte Carlo calculations.

(6) Small-cluster studies have shown that the momentum of a doped carrier takes a value close to the Fermi surface.[12] This fact has also been checked by the case with one doped hole in the one-dimensional Hubbard model.[20] Here we reconsider this problem using the explicit form of the wave function in the large-$U$ limit. Let us consider the case with $M=$even and $N=$odd ($N=N_A-1$, $M=N_A/2$) for the one-hole case. Then both $I_j$'s and $J_\alpha$'s are integers

$$I_j=\left\{-\frac{N-1}{2},-\frac{N-3}{2},\ldots,-1,0,1,\ldots,\frac{N-3}{2},\frac{N-1}{2}\right\},$$

$$J_\alpha=\left\{-\frac{M-2}{2},-\frac{M-4}{2},\ldots,-1,0,1,\ldots,\frac{M-2}{2},\frac{M}{2}\right\},$$

or

$$J_\alpha=\left\{-\frac{M}{2},-\frac{M-2}{2},\ldots,-1,0,1,\ldots,\frac{M-4}{2},\frac{M-2}{2}\right\}. \tag{5.2}$$

In this case

$$k_j=\frac{2\pi}{L}\left[I_j\pm\frac{M}{2N}\right], \tag{5.3}$$

and thus the total momentum is

$$K=\sum_j k_j=\pm\pi M/L=\pm\pi/2\ ,$$

and the total energy is

$$\begin{aligned}E&=-2t\sum_{j=1}^{N}\cos k_j\\&=-2t\sum_{j=1}^{N}\cos\left[\frac{2\pi I_j}{N_A}\right]\cos\left[\frac{\pi M}{NN_A}\right]\\&=-2t\cos\left[\frac{\pi}{2N}\right].\end{aligned} \tag{5.4}$$

We can interpret the total momentum and energy by assuming an effective hopping amplitude of the doped hole. When the system is translated by the unit lattice constant, the spin part of the wave function $\Phi(y_1,\ldots,y_M)$ is replaced by[21]

$$\begin{aligned}\Phi(y_1+1,\ldots,y_M+1)&=(-1)^M\exp\left[-i\sum_\alpha\theta(2\Lambda_\alpha)\right]\\&\quad\times\Phi(y_1,\ldots,y_M)\\&=\exp\left[\pm\frac{i\pi M}{N}\right]\Phi(y_1,\ldots,y_M)\ .\end{aligned} \tag{5.5}$$

We may consider that this phase factor $\exp(\pm i\pi M/N)$ is due to a "gauge" potential induced by the surrounding spin system.[22] (In this case it is one-dimensional Heisenberg system.) Using this phase factor and assuming that the effective hopping amplitude of a doped hole is given by

$$-t\exp\left[\pm\frac{i\pi M}{N}\right],$$

we can readily see that the lowest-energy state of the doped hole has a finite momentum $K=\pm\pi/2$ and its kinetic energy becomes

$$-2t\cos\left[\pm\frac{\pi M}{N}-K\right]=-2t\cos\left[\frac{\pi}{2N}\right],$$

which reproduces the exact result.

## ACKNOWLEDGMENTS

The authors wish to thank S. Sorella, Y. Hatsugai, and M. Imada for useful discussions. One of the authors (H.S.) expresses his thanks to E. Pytte and D. H. Lee for their hospitality at IBM Yorktown Heights, where a part of this work was carried out. This work is supported in part by a Grant-in-Aid of Scientific Research from the Ministry of Education, Science and Culture, Japan.

## APPENDIX A

Let us prove in this appendix that the wave function Eq. (2.14) gives the correct energy up to the order of $t/U$. In the large-$U$ limit one can rewrite the Hubbard model as[14,23]

$$\tilde{H}=-t\sum_{(i,j)\sigma}(a_{i\sigma}^{\dagger}a_{j\sigma}+\text{H.c.})+2J\sum_{(i,j)}(\mathbf{S}_i\cdot\mathbf{S}_j-\tfrac{1}{4}n_in_j)+\frac{J}{2}\sum_{(i,j)(i,j')j\neq j'\sigma}(a_{i\sigma}^{\dagger}a_{i-\sigma}a_{j-\sigma}^{\dagger}a_{j'\sigma}-n_{i-\sigma}a_{j\sigma}^{\dagger}a_{j'\sigma}), \tag{A1}$$

where $J=2t^2/U$ and $a_{j\sigma}\equiv c_{j\sigma}(1-n_{j-\sigma})$. The expectation value of each term with respect to (2.14) is as follows.

(1) The first term gives $E_1=-2t\sum_j\cos k_j$ as described in Sec. II. In the limit of $N_A\to\infty$, we have

$$E_1=-\frac{2tN_A}{\pi}\sin n\pi, \tag{A2}$$

with $n=N/N_A=2k_F/\pi$.

(2) The second term of Eq. (A1) is nonvanishing only when both of the nearest-neighbor sites $(i,j)$ are occupied. The possibility of this case is independent of the spin configuration so that it is given by

$$\langle n_in_{i+1}\rangle_{\mathrm{SF}}=n^2-\frac{\sin^2 n\pi}{\pi^2}, \tag{A3}$$

where $\langle\ \rangle_{\mathrm{SF}}$ indicates an expectation value within the spinless fermion system. Once nearest-neighbor sites are occupied, $\mathbf{S}_i\cdot\mathbf{S}_j$ has a value equal to the exchange energy in the Heisenberg model. Using the well-known result of the Heisenberg chain,[6] we have

$$E_2=-2(\ln 2)N_AJ\left[n^2-\frac{\sin^2 n\pi}{\pi^2}\right]. \tag{A4}$$

(3) The third term of Eq. (A1) causes two changes in the wave function. First, the Slater determinant changes. This effect is again independent of the spin configurations and can be taken into account by

$$\langle n_ia_j^{\dagger}a_{j'}\rangle_{\mathrm{SF}}=n\frac{\sin 2n\pi}{2\pi}-\frac{\sin^2 n\pi}{\pi^2}, \tag{A5}$$

for each combination of $(i,j,j')$. Secondly, the spin wave function also changes. We can easily see that it changes in a similar way as the exchange interaction but with an opposite sign. Therefore with respect to the spin degrees of freedom, we have $(\ln 2)J$ for each set of $(i,j,j')$. Counting the number of combination $(i,j,j')$, we obtain

$$E_3=2(\ln 2)N_AJ\left[n\frac{\sin 2n\pi}{2\pi}-\frac{\sin^2 n\pi}{\pi^2}\right]. \tag{A6}$$

Summing up all these energies, we have

$$E/N_A=-\frac{2t}{\pi}\sin n\pi-4(\ln 2)\frac{t^2}{U}n^2\left[1-\frac{\sin 2n\pi}{2n\pi}\right], \tag{A7}$$

which agrees with the exact result up to the order of $t/U$.[24]

## APPENDIX B

Here we sketch the lowest-order perturbation calculation in terms of $U$ to look into the singularities of $n(k)$ and $S(k)$. The ground-state wave function $\psi$ is expanded as

$$\psi=\psi^{(0)}+\psi^{(1)}+\cdots,$$

$$\psi^{(0)}=|0\rangle,$$

$$\psi^{(1)}=-\frac{1}{N}\sum_{k,k',q}\frac{U}{\varepsilon_k+\varepsilon_{k'-k+q}-\varepsilon_{k'}-\varepsilon_q}c_{k\uparrow}^{\dagger}c_{k'-k+q\downarrow}^{\dagger}c_{k'\downarrow}c_{q\uparrow}|0\rangle,$$

where $\varepsilon_k=-2t\cos k$ and $|0\rangle$ denotes the Fermi sea.

Taking the expectation value over $\psi$, we easily obtain from Eq. (3.4) the following lowest correction to the momentum distribution function:

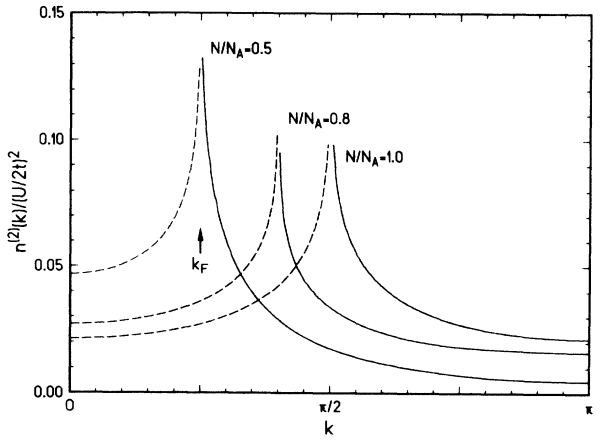


FIG. 12. The lowest-order correction to the momentum distribution, $n^{(2)}(k)$, evaluated with the perturbation calculation in terms of $U$. $N/N_A=\frac{1}{2}$ (the quarter-filled case), $N/N_A=0.8$, and $N/N_A=1$ (the half-filled case) are chosen. $n^{(2)}(k)$ for $k>k_F$ ($k<k_F$) are shown by solid (dashed) lines. At $k=k_F$ they have a logarithmic singularity as shown in (B3).

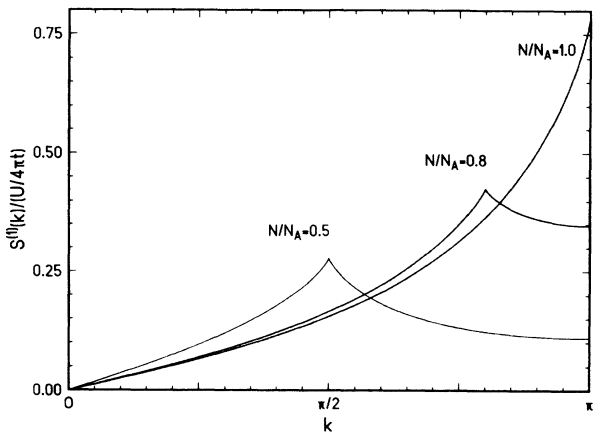


FIG. 13. The lowest-order correction to the spin-correlation function, $S^{(1)}(k)$, which has been evaluated with the perturbation calculation in terms of $U$ for the electron densities $N/N_A=0.5$, 0.8, and 1.0.

$$n^{(2)}(k)=U^2\frac{1}{N^2}\sum_{q,k'}\frac{f(\varepsilon_{k'})f(\varepsilon_q)[1-f(\varepsilon_{k'-k+q})]}{(\varepsilon_k+\varepsilon_{k'-k+q}-\varepsilon_q-\varepsilon_{k'})^2}\ , \tag{B1}$$

for $k>k_F$ and

$$n^{(2)}(k)=-U^2\frac{1}{N^2}\sum_{q,k'}\frac{f(\varepsilon_{k'})[1-f(\varepsilon_q)][1-f(\varepsilon_{k'-k+q})]}{(\varepsilon_{k'-k+q}+\varepsilon_q-\varepsilon_k-\varepsilon_{k'})^2}\ , \tag{B2}$$

for $k<k_F$. Here $f(\varepsilon)$ represents the Fermi distribution function.

The contributions singular at $k=k_F$ come from the regions where all the energies involved are close to the Fermi energy. A straightforward calculation from (B1) and (B2) leads to

$$n^{(2)}(k)\simeq\pm C\left[\frac{U}{4\pi t\sin k_F}\right]^2\ln\frac{k_F}{|k-k_F|}\ , \tag{B3}$$

where + or − should be taken in accordance with the sign of $k-k_F$. $C$ is $\frac{1}{2}$ for the less-than-half-filled case or $\frac{3}{4}$ for the half-filled case. The extra factor of $\frac{1}{4}$ in the latter case is due to the umklapp term, which contributes equally to the singularity.

As (B1) shows, the momentum distribution function has a weak singularity at $k=3k_F$, since the electron near $k_F$ can be excited to a state around $3k_F$ together with an electron-hole pair excitation having its momentum near $-2k_F$. In fact, it is easy to see that $\partial^2 n^{(2)}(k)/\partial k^2$ has a jump at $k=3k_F$.

Similarly $S(k)$ can be evaluated with Eq. (4.1). The first correction to the unperturbed value

$$S^{(0)}(k)=\begin{cases}\frac{1}{4}\frac{k}{\pi} & \text{for } k<2k_F\ ,\\ \frac{1}{4}\frac{2k_F}{\pi} & \text{for } k>2k_F\ ,\end{cases} \tag{B4}$$

is linear in $U$ as

$$S^{(1)}(k)=\frac{U}{N^2}\sum_{k_1,k_2}\frac{f(\varepsilon_{k_1})f(\varepsilon_{k_2})[1-f(\varepsilon_{k_1-k})][1-f(\varepsilon_{k_2+k})]}{\varepsilon_{k_1-k}+\varepsilon_{k_2+k}-\varepsilon_{k_1}-\varepsilon_{k_2}}\ . \tag{B5}$$

Again from the regions where all the $\varepsilon$'s in (B5) are close to the Fermi energy, the singularity at $2k_F$ is obtained as

$$S^{(1)}(k)\simeq\frac{U}{16\pi^2 t\sin k_F}\left[\text{const}-|k-2k_F|\ln\frac{k_F}{|k-2k_F|}\right]\ . \tag{B6}$$

The $k$ dependence of both $n^{(2)}(k)$ and $S^{(1)}(k)$ is shown, respectively, in Figs. 12 and 13 for various densities.

*Address until September 1990: Theoretische Physik, ETH-Hönggerberg, CH-8093 Zürich, Switzerland.

†Present address: Department of Physics, Tokyo Institute of Technology, Oh-okayama, Tokyo 152, Japan.

[1]See, for instance, P. W. Anderson, in *Frontiers and Borderlines in Many Particle Physics*, proceedings of the International School of Physics "Enrico Fermi," 1987 (North-Holland, Amsterdam, in press); P. W. Anderson, Science **235**, 1196 (1987).

[2]V. Emery, Phys. Rev. Lett. **58**, 2794 (1987).

[3]F. C. Zhang and T. M. Rice, Phys. Rev. B **37**, 3759 (1988).

[4]E. H. Lieb and F. Y. Wu, Phys. Rev. Lett. **20**, 1445 (1968); C. N. Yang, *ibid.* **19**, 1312 (1967).

[5]See, for instance, H. Shiba, Phys. Rev. B **6**, 930 (1972); M. Takahashi, Prog. Theor. Phys. **47**, 69 (1972); J. Carmelo and D. Baeriswyl, Phys. Rev. B **37**, 7541 (1988); N. Kawakami, T. Usuki, and A. Okiji, Phys. Lett. A **137**, 287 (1989).

[6]H. Bethe, Z. Phys. **71**, 205 (1931); L. Hulthén, Arkiv. Mat. Astron. Fys. **26A**, No. 11 (1938).

[7]B. Doucot and X. G. Wen, Phys. Rev. B **40**, 2719 (1989).

[8]S. Sorella, E. Tosatti, S. Baroni, R. Car, and M. Parrinello, *Progress in High Temperature Superconductivity* (World Scientific, Singapore, 1988), Vol. 14, p. 457.

[9]J. Sólyom, Adv. Phys. **28**, 201 (1979).

[10]J. E. Hirsch and D. J. Scalapino, Phys. Rev. B **27**, 7169 (1983).

[11]R. J. Birgeneau, Y. Endoh, K. Kakurai, Y. Hidaka, T. Murakami, M. A. Kastner, T. R. Thurston, G. Shirane, and K. Yamada, Phys. Rev. B **39**, 2868 (1989).

[12]M. Ogata and H. Shiba, J. Phys. Soc. Jpn. **58**, 2836 (1989); E. Kaxiras and E. Manousakis, Phys. Rev. B **38**, 866 (1988); E. Dagotto, A. Moreo, and T. Barnes, Phys. Rev. B **40**, 6721 (1989); J. Bonča, P. Prelovšek, and I. Sega, *ibid.* **39**, 7074 (1989); Y. Hasegawa and D. Poilblanc, *ibid.* (to be published).

[13]T. Oguchi, H. Nishimori, and Y. Taguchi, J. Phys. Soc. Jpn. **55**, 323 (1986).

[14]C. Gros, R. Joynt, and T. M. Rice, Phys. Rev. B **36**, 381 (1987).

[15]M. Imada and Y. Hatsugai, J. Phys. Soc. Jpn. **58**, 3752 (1989).

[16]K. Kubo, T. A. Kaplan, and J. R. Borysowicz, Phys. Rev. B **38**, 11 550 (1988).

[17]B. I. Shraiman and E. D. Siggia, Phys. Rev. Lett. **61**, 467 (1988); C. Kane, P. A. Lee, and N. Read, Phys. Rev. B **39**, 6880 (1989).

[18]If we take $g_2$ as the fixed point value $g_2^* = U/2$, $\alpha$ is smaller.

[19]S. Sorella (private communication).

[20]M. Ogata and H. Shiba, in Ref. 12.

[21]This relation holds even in the case where $y_M = N$ and the translation results in an arrangement of $y_i$'s.

[22]R. B. Laughlin, Phys. Rev. Lett. **60**, 2677 (1988); Science **242**, 525 (1988); P. A. Lee, Phys. Rev. Lett. **63**, 680 (1989); R. Shanker, *ibid.* **63**, 203 (1989).

[23]K. A. Chao, J. Spalek, and A. M. Olés, J. Phys. **10C**, L271 (1977); J. E. Hirsch, Phys. Rev. Lett. **54**, 1317 (1985); H. Yokoyama and H. Shiba, J. Phys. Soc. Jpn. **57**, 2482 (1988).

[24]H. Shiba, in Ref. 5.